THE ASTROPHYSICAL JOURNAL, 445:591–598, 1995 June 1

INNER TWO-ARM SYMMETRY IN SPIRAL GALAXIES

DEBRA MELOY ELMEGREEN[1] AND BRUCE G. ELMEGREEN[2]
Received 1994 August 25; accepted 1994 December 8

ABSTRACT

Most galaxies with spiral density waves, including those with multiple long arms, have two prominent symmetric arms in their inner regions, inside $\sim 0.5R_{25}$. Grand-design galaxies, which have two prominent arms throughout their disks, also have brighter, narrower, and more continuous arms inside this radius. Based on measurements of these morphological features in 173 spiral galaxies, and on our previous studies of optical resonance indicators, we propose that corotation is optically visible in most spiral galaxies and is located near the radius of the endpoints of the highly symmetric part of the spiral arms, approximately midway out in the disk. This places the outer Lindblad resonance at $\sim R_{25}$, or ~ 4 scale lengths, for most spiral galaxies. In barred galaxies, the two inner symmetric arms end at twice the bar radius, independent of the bar type. If large bars end near corotation, then the ends of the two prominent arms must be beyond corotation in these systems.

Subject headings: galaxies: kinematics and dynamics — galaxies: structure

1. INTRODUCTION

Grand-design and multiple-arm galaxies have two-arm symmetric structures in at least the inner parts of their disks (Elmegreen & Elmegreen 1982, 1987). In a grand-design galaxy, these two arms extend all of the way from the inner region to the outer optical edge. In a multiple-arm galaxy, the inner two arms branch midway out in the disk, and there are other arms as well. We show here that in most galaxies, including grand-design galaxies, there is usually a change in the appearance of the spirals midway out in the disk because of symmetric bifurcations or broadenings of the arms.

Four examples of these middisk changes are evident in Figure 1. In NGC 895, there are two bright spiral arms that fade abruptly at $\sim 1'$ from the nucleus at the top and bottom of the image. Both arms broaden and bifurcate at this point, and then continue further out as fainter spirals; other arms are present too. In NGC 1566, there is a bright inner spiral extending for $\sim 2'$ which then becomes very broad, and there are also several faint outer arms. In NGC 2997, there are two broad main arms in the inner region which bifurcate at $\sim 3'$ on the left and right in the image. In NGC 7412, the two prominent inner arms bifurcate at $\sim 1'$ on the left and top. These arm structures are present in most spiral galaxies, including those with bars.

Long spiral arms like these are generally thought to be caused by density waves (Lin & Shu 1964). We speculate that middisk broadenings and bifurcations such as those present in Figure 1 result from resonant interactions between the wave and stellar motions in the disk and from a lack of strong coherence between the stellar spiral potential and stellar orbits beyond corotation.

Several methods for determining the resonance radii of spiral waves in nonbarred galaxies have been proposed recently, based on optical morphology (Elmegreen, Elmegreen, & Seiden 1989, hereafter EES; Elmegreen & Elmegreen 1990; Elmegreen, Elmegreen, & Montenegro 1992, hereafter EEM; Buta & Crocker 1991; Buta 1994), star formation patterns (Cepa & Beckman 1990a, b), gas kinematics (Westpfahl 1995; Canzian 1993), gasdynamical modeling (Garcia-Burillo, Combes, & Gerin 1993; Garcia-Burillo, Sempere, & Combes 1994; Sempere, Garcia-Burillo, & Combes 1995) and mode fitting (Lowe et al. 1994). All of these methods agree for the few galaxies that they have in common (M81, M100, and M51), and they all suggest that corotation is midway out in the optical disk, at about $(0.4–0.6)R_{25}$, where R_{25} is the radius at which the surface brightness is 25 mag arcsec^{-2} (not to be confused with log R_{25} in the RC3, which measures the axial ratio). These results suggest that the termination radii of the prominent inner two-arm spirals could be a manifestation of corotation. The connection between corotation and middisk arm bifurcations was previously noted for two galaxies (Cepa & Beckman 1990a), and discussed theoretically by Saslaw (1985).

Here we study the deprojected radii of the middisk bifurcations in 173 barred and nonbarred spiral galaxies. Section 2 presents the data, § 3 discusses correlations with absolute galaxy magnitudes and Hubble types, and § 4 summarizes the implications for spiral wave resonances.

2. DATA

All barred and nonbarred spiral galaxies in the Atlas of Galaxies (Sandage & Bedke 1988), the Revised Shapley-Ames Catalog of Bright Galaxies (Sandage & Tammann 1981; hereafter RSA), and the Hubble Atlas (Sandage 1961) were examined for inner two-arm spiral structure. These atlases include most spiral galaxies with inclinations less than 60° and radii greater than 2.'5, as listed in the Third Reference Catalogue of Bright Galaxies (de Vaucouleurs et al. 1991; hereafter RC3). The 24 galaxies with radii greater than 2.'5 that are not in the high-resolution atlases were examined on the blue prints of the Palomar Observatory Sky Survey (POSS). Several galaxies in the total sample were eliminated because their spiral structure was flocculent (so they did not have two symmetric inner arms; 35 galaxies), or they did not have magnitudes listed in Tully (1988) nor in the RC3 (11 galaxies), or the POSS image was overexposed in the central region (for three galaxies not in an atlas). Twenty galaxies that had been previously classified as flocculent based on the POSS images (Elmegreen & Elmegreen

[1] Vassar College Observatory, Box 278, Poughkeepsie, NY 12601.
[2] IBM T. J. Watson Research Center, P.O. Box 218, Yorktown Heights, NY 10598.

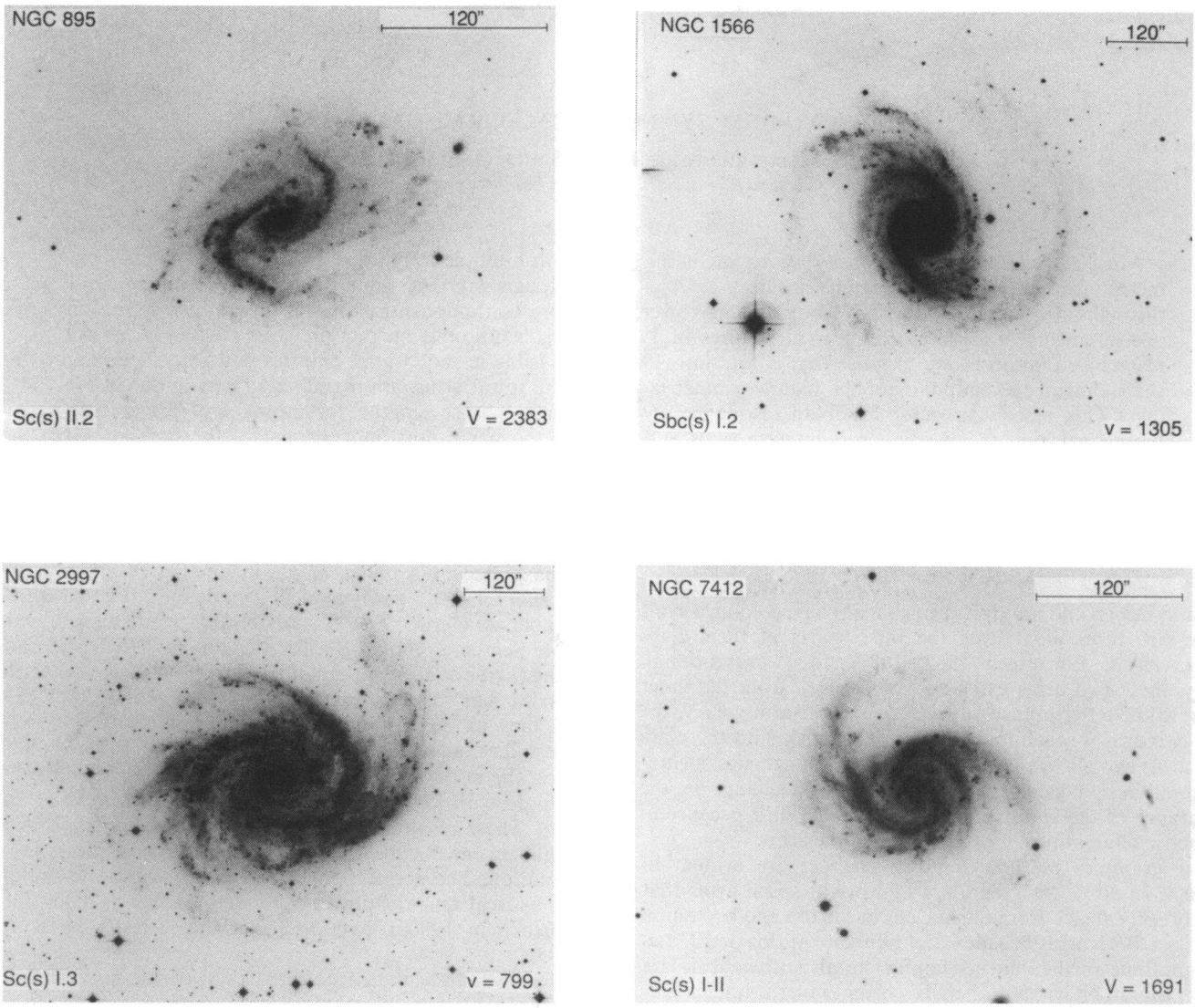

FIG. 1.—NGC 895, NGC 1566, NGC 2997, and NGC 7412 reproduced from the Sandage & Bedke atlas show two inner arms which form a ridge and then bifurcate at the termination of the ridge.

1987) are included here because they show two-arm symmetry on the Sandage & Bedke photographs.

For the 173 galaxies in our final sample, the positions of the endpoints of each arm in the inner two-arm structure were measured and their radii were determined by correcting for inclination. These endpoints are where the arms bifurcate or broaden. When an arm bifurcates, a second arm typically comes off of it at a relative pitch angle of $\sim 30°$ and continues to spiral around the center for an additional 90°–270° in azimuth.

Tables 1–3 list the measured galaxies in this sample, arranged according to NGC number and divided among the tables according to bar type: SA (46 total) in Table 1, SAB (73 total) in Table 2, and SB (54 total) in Table 3. Also listed are the Hubble types (from the RC3), arm classes AC (Elmegreen & Elmegreen 1987), absolute blue magnitudes M_B (Tully 1988; we used apparent magnitudes and velocities from RSA with $H_0 = 75$ km s^{-1} kpc^{-1} to determine M_B for 11 galaxies not in Tully), measured endpoints of the inner two arms with radii $R_{\rm arm\,1}$ and $R_{\rm arm\,2}$ in arcminutes and angles θ_1 and θ_2 measured counterclockwise from the major axis, average inclination-corrected inner two-arm radii, $R_{\rm arm}$, divided by R_{25}, and deprojected relative bar radius $R_{\rm bar}/R_{25}$ for the SB galaxies. The radius R_{25} was determined from the corrected diameter D_0 given in the RC3. Galaxies with prominent star formation ridges in the inner two-arm spirals are indicated. The major axes were determined by eye because the orientations of the images in the photographic atlases are arbitrary. The angles between the spiral-arm endpoints and the major axes are estimated to be accurate to $\pm 5°$, which gives a 4% uncertainty in the corrected radii of the arms for the most inclined galaxies with the least favorable arm orientations.

The inner two arms are symmetric in the sense that they have the same length to within 20% for most of the galaxies, independent of Hubble type, bar type, and arm class. Figure 2*a* shows a histogram of the relative difference in the corrected length of the two arms, $|R_{\rm arm\,1} - R_{\rm arm\,2}|/[0.5(R_{\rm arm\,1} + R_{\rm arm\,2})]$. The average lengths for the arms were used for the correlations

TABLE 1

INNER TWO ARMS FOR SA GALAXIES

NGC	Type	AC	M_B	$R_{arm\,1}$	θ_1	$R_{arm\,2}$	θ_2	R_{arm}/R_{25}	Ridge
300	7	5	−16.88	3.71	160°	3.23	345°	0.31	Yes
598	6	5	−18.31	8.66	10	8.47	182	0.23	Yes
628	5	9	−20.32	1.41	0	1.55	180	0.28	
895	6	9	−20.11	1.08	70	0.92	215	0.55	Yes
1084	5	5	−20.26	0.41	25	0.41	205	0.28	
1288	4	9	−22.42	0.76	25	0.66	180	0.62	
1357	2	12	−19.62	0.56	40	0.56	280	0.58	Yes
1494	7	5	−18.53	0.68	30	0.60	205	0.41	
2280	6	9	−21.03	0.84	40	0.68	220	0.20	Yes
2942	5	9	−22.23	0.38	20	0.26	180	0.28	
2967	5	9	−20.31	0.38	60	0.35	240	0.23	
3031	2	12	−18.29	5.26	165	6.10	345	0.41	
3241	2	3	−19.64	0.45	15	0.45	192	0.37	
3294	5	9	−20.19	0.65	35	0.79	217	0.43	Yes
3338	5	9	−20.80	1.01	5	0.91	180	0.32	
3423	6	2	−18.68	0.75	160	0.71	340	0.37	
3433	5	9	−20.58	0.51	150	0.54	345	0.30	Yes
3511	5	2	−20.15	1.03	160	1.02	0	0.34	
3631	5	9	−20.69	1.15	160	0.97	320	0.42	
3642	4	9	−20.66	0.71	15	0.62	200	0.23	
3684	4	5	−19.69	0.54	10	0.64	195	0.38	
3810	5	2	−20.11	1.09	35	0.81	190	0.44	
3938	5	9	−20.26	0.60	80	0.49	260	0.20	
4254	5	9	−20.84	2.05	285	1.61	85	0.68	
4504	6	5	−19.95	0.90	0	0.87	200	0.51	
4603	5	9	−21.93	0.71	150	0.83	330	0.40	Yes
4651	5	9	−20.07	0.36	30	0.32	200	0.17	
4775	7	9	−20.32	0.35	50	0.42	260	0.35	
4939	4	12	−22.43	1.13	50	1.53	240	0.47	
5033	5	9	−21.03	2.11	58	2.25	228	0.42	
5054	4	5	−21.18	1.58	350	1.45	8	0.58	
5085	5	2	−20.71	0.63	100	0.63	280	0.37	Yes
5161	5	9	−21.12	1.28	130	1.05	300	0.40	
5194	4	12	−20.75	2.20	20	2.57	220	0.42	Yes
5247	4	9	−20.95	2.15	55	1.87	200	0.49	Yes
5351	3	9	−22.07	0.68	310	0.47	90	0.39	
5364	4	9	−21.17	1.95	95	1.83	290	0.55	
5483	5	5	−20.26	0.85	300	0.76	120	0.41	Yes
5494	5	5	−21.21	0.44	0	0.56	180	0.42	
6015	6	5	−20.05	1.06	70	1.10	260	0.40	
6070	6	9	−20.72	0.58	35	0.66	260	0.32	
6118	6	9	−20.62	0.80	280	0.89	90	0.33	
6643	5	5	−20.79	0.57	150	0.80	290	0.35	
6753	3	8	−22.64	1.03	20	0.97	200	0.78	
IC 2627	4	12	−20.05	0.66	30	0.73	205	0.36	Yes
IC 5332	7	9	−18.45	0.73	310	0.80	90	0.23	

described below. In Figure 2*b*, a histogram of the difference in angle between arm 1 and arm 2, rotated 180°, shows that most arms are within 20° of being 180° apart.

3. RESULTS

Figures 3 and 4 plot R_{arm}/R_{25} versus the absolute blue magnitude M_B for SA and SAB galaxies, respectively. The normalization to R_{25} is an attempt to scale out the large variations from galaxy to galaxy based on intrinsic size or distance; typically, R_{25} is ~4 exponential scale lengths (i.e., for a constant extrapolated central surface brightness). We also found in our earlier studies (EES; EEM) that R_{25} was approximately the location of the outer Lindblad resonance (OLR), to within 10%.

The solid lines in Figures 3 and 4 represent the ratio of the corotation resonance to the OLR, and the long-dashed lines are the ratio of the inner 4 : 1 resonance to the OLR. These ratios of resonance radii were determined from a magnitude-dependent fit to the slope of the rotation curve using the results of Persic & Salucci (1991). As shown in EEM, the ratio of any resonance radius, R_{res}, to the corotation radius, R_{CR}, is given by

$$R_{res}/R_{CR} = [1 - (2/m)(1 + \alpha)^{0.5}]^{1/(1-\alpha)}$$

for a power-law fit to a rotation curve, $v(R) \sim R^{\alpha}$; here $m = 2$ for the inner 2:1 (i.e., Lindblad) resonance (ILR), $m = -2$ for the OLR, etc. The power is given by $\alpha = \log [(2.2 + \Delta)/(2.2 - 1.2\Delta)]/\log 3.2$, where $\Delta = 0.12 + 0.096(M_B + 21.5)$ for absolute magnitude M_B. The theoretical lines in the plots of radius versus magnitude are $R_{arm}/R_{25} \cong -0.05M_B +$ constant.

Despite the wide scatter in the data in Figures 3 and 4 and the approximation used for the rotation curves, there is a suggestion that the inner two-arm structures end near corotation at a radius that scales in the proper way with galaxy size if the OLR is close to R_{25}. The results are independent of arm class.

The short-dashed lines in Figures 3 and 4 are linear least-squares fits to these data. For Figure 3, the slope of the fit is

TABLE 2

INNER TWO ARMS FOR SAB GALAXIES

NGC	Type	AC	M_B	$R_{arm\,1}$	θ_1	$R_{arm\,2}$	θ_2	R_{arm}/R_{25}	Ridge
157	4	12	−20.85	0.52	0°	0.60	180°	0.26	Yes
210	3	6	−20.06	1.61	30	1.87	335	0.70	
255	4	2	−19.26	0.58	130	0.64	300	0.40	
514	5	9	−20.24	0.53	310	0.44	90	0.28	
578	5	9	−20.09	0.88	0	0.78	180	0.34	
685	5	9	−19.02	0.79	135	0.85	340	0.44	
753	4	9	−21.79	0.38	20	0.45	195	0.32	
864	5	5	−20.20	0.93	40	0.93	220	0.39	
918	5	12	−19.44	0.62	37	0.78	143	0.51	Yes
925	7	1	−19.66	2.85	38	2.65	264	0.50	Yes
1042	6	9	−19.91	0.63	40	0.51	175	0.24	
1232	5	9	−21.11	1.27	110	1.18	300	0.33	
1566	4	12	−20.45	1.73	25	1.56	195	0.40	Yes
1637	5	5	−18.33	0.50	140	0.63	300	0.28	Yes
2223	3	9	−20.85	0.70	80	0.88	265	0.48	
2336	4	9	−22.00	1.04	340	1.39	142	0.35	
2776	5	9	−20.77	0.37	30	0.37	210	0.25	
2848	5	2	−19.78	0.51	5	0.60	180	0.39	
2903	4	7	−19.85	2.27	280	2.83	110	0.41	
2935	3	8	−21.74	1.34	345	1.25	150	0.70	
2997	5	9	−20.74	2.05	350	2.20	160	0.42	
3001	4	9	−20.36	0.67	170	0.75	10	0.44	
3054	3	9	−20.55	0.83	150	0.60	340	0.35	
3124	4	9	−21.35	0.57	20	0.51	220	0.35	
3184	6	9	−19.34	1.34	70	1.37	245	0.37	
3344	4	9	−18.47	1.39	25	1.21	182	0.37	
3464	4	9	−21.08	0.41	280	0.40	110	0.30	
3486	5	9	−18.61	1.06	22	1.46	235	0.36	
3596	5	5	−20.31	0.39	300	0.32	110	0.18	
3614	5	5	−20.91	0.70	60	0.61	220	0.29	
3705	2	5	−20.15	0.91	20	1.24	200	0.43	
3726	5	5	−20.35	0.77	150	0.91	330	0.27	
3756	4	9	−19.96	0.75	40	0.60	190	0.32	
3893	5	12	−20.27	0.65	50	0.56	210	0.27	Yes
4051	4	5	−20.25	1.54	135	1.17	320	0.52	
4136	5	9	−18.23	0.77	20	0.84	185	0.40	
4145	7	4	−20.21	1.54	2	1.63	195	0.54	
4214	9	2	−17.57	1.30	35	1.56	220	0.34	
4303	4	9	−20.71	1.28	330	1.33	170	0.40	
4321	4	12	−21.13	1.81	290	2.08	100	0.51	Yes
4487	6	5	−20.19	0.76	50	0.77	220	0.37	
4535	5	9	−20.60	1.20	20	1.46	210	0.38	
4536	4	12	−20.02	1.24	0	1.12	200	0.31	
4559	6	4	−20.07	1.46	330	1.59	155	0.28	
4579	3	9	−20.67	1.44	315	1.39	95	0.53	
4653	6	5	−20.19	0.42	40	0.50	200	0.30	
4725	2	6	−20.65	2.14	28	1.92	215	0.37	
4891	4	9	−20.29	0.76	80	0.60	260	0.52	
4899	5	4	−20.82	0.38	0	0.27	180	0.25	
4981	4	4	−20.42	0.62	345	0.66	150	0.47	
5068	6	2	−18.93	1.21	90	1.28	270	0.32	
5236	5	9	−20.31	2.44	230	3.83	70	0.48	Yes
5248	4	12	−21.07	1.73	30	1.81	210	0.57	Yes
5371	4	9	−21.57	0.71	156	0.78	311	0.34	
5457	6	9	−20.45	2.55	0	3.15	190	0.20	
5468	6	9	−21.09	0.45	50	0.47	345	0.34	
5584	6	5	−20.29	0.58	330	0.56	250	0.33	
5605	5	5	−20.41	0.27	130	0.27	300	0.31	
5660	5	9	−20.60	0.40	0	0.42	180	0.30	
5669	6	5	−19.88	1.14	190	1.17	20	0.57	
5861	5	12	−20.80	0.68	140	0.85	0	0.46	
5885	5	5	−20.75	0.41	30	0.55	185	0.24	
5985	3	9	−21.42	0.87	0	0.75	180	0.30	
6181	5	12	−20.92	0.80	290	0.60	100	0.55	
6384	4	9	−21.31	1.78	80	1.32	270	0.46	
6744	4	5	−21.39	3.44	47	4.18	265	0.37	
6814	4	9	−20.41	0.47	340	0.31	170	0.23	
6946	6	9	−20.78	2.77	0	2.23	190	0.30	
6951	4	12	−20.73	1.45	40	1.13	210	0.54	Yes
7125	5	9	−20.25	1.03	65	0.44	205	0.48	
7418	6	9	−19.43	0.76	50	0.82	200	0.44	
7424	6	9	−19.55	1.71	66	1.34	187	0.32	Yes
7678	5	5	−21.17	0.63	150	0.64	270	0.52	

TABLE 3

INNER TWO ARMS FOR SB GALAXIES

NGC	Type	AC	M_B	$R_{arm\,1}$	θ_1	$R_{arm\,2}$	θ_2	R_{arm}/R_{25}	R_{bar}/R_{25}	Ridge
					Large Bar					
613	4	9	−20.53	1.'63	5°	1.'71	190°	0.61	0.37	Yes
1097	3	12	−20.79	3.77	70	4.04	253	0.82	0.28	Yes
1300	4	12	−20.42	1.46	35	1.69	230	0.50	0.35	Yes
1365	3	12	−21.26	4.8	185	4.9	355	0.86	0.35	
1433	2	6	−19.67	3.5	80	3.4	310	0.59	0.46	
1672	3	5	−19.84	3.01	90	3.18	260	0.96	0.42	
3513	5	12	−19.46	0.96	200	1.03	5	0.69	0.28	
4123	5	9	−20.25	0.81	110	1.15	300	0.45	0.30	
4304	4	9	−20.97	1.13	100	19	300	0.77	0.33	
4548	3	12	−20.28	2.24	0	1.77	180	0.73	0.33	Yes
4593	3	5	−21.58	1.46	30	1.43	230	0.74	0.33	
4597	9	1	−19.15	0.65	190	0.82	10	0.73	0.30	
5383	3	12	−20.96	1.14	90	0.87	260	0.67	0.50	
5398	8	5	−19.01	1.11	157	0.81	327	0.65	0.32	
6217	4	5	−20.19	0.64	10	0.74	240	0.52	0.30	
7479	5	9	−21.11	1.23	63	1.77	258	0.70	0.38	
7552	2	7	−20.14	0.97	30	1.95	235	0.84	0.51	
					Small Bar					
151	4	9	−21.82	0.69	35	0.81	230	0.40	0.24	
289	4	12	−19.94	1.15	170	1.66	290	0.53	0.10	
1073	5	5	−19.44	1.14	255	0.98	50	0.43	0.16	
1187	5	9	−19.76	0.86	10	0.80	180	0.30	0.073	
1313	3	5	−18.60	1.64	43	2.12	250	0.44	0.20	
1398	2	6	−20.57	1.06	55	1.13	250	0.33	0.21	
1493	6	5	−18.47	0.69	110	0.84	260	0.44	0.17	
1744	7	4	−18.06	2.25	160	2.06	320	0.53	0.19	
1784	5	2	−20.37	1.10	250	0.60	30	0.39	0.20	
2525	5	6	−19.89	1.15	60	0.99	245	0.74	0.20	
2713	2	12	−21.59	1.31	18	1.31	200	0.69	0.15	
2763	6	9	−19.53	0.63	130	0.46	300	0.45	0.094	
2835	5	9	−19.66	0.98	200	1.00	50	0.30	0.20	
3059	4	5	−19.75	1.05	95	0.89	290	0.60	0.15	
3198	5	7	−19.62	1.63	20	1.19	190	0.34	0.034	
3319	6	5	−18.71	1.13	40	1.07	175	0.80	0.22	
3346	6	9	−19.35	0.42	120	0.45	310	0.30	0.13	
3347	3	12	−20.81	0.58	155	0.58	335	0.26	0.15	
3351	3	6	−19.26	0.76	40	0.86	220	0.21	0.11	
3359	5	5	−20.59	1.44	55	1.73	250	0.44	0.13	
3367	5	9	−21.21	0.51	85	0.46	265	0.41	0.23	
3485	3	2	−19.10	0.57	70	0.71	220	0.56	0.26	
3673	3	5	−20.20	0.64	60	0.75	290	0.39	0.14	
3686	4	5	−19.94	0.79	115	0.62	335	0.44	0.13	
3887	4	2	−19.91	0.82	40	0.85	230	0.50	0.18	
3992	4	9	−20.75	1.90	85	1.93	240	0.51	0.21	
4394	3	6	−19.49	0.85	45	0.83	240	0.43	0.29	
5334	5	2	−19.66	0.55	30	0.57	220	0.26	0.074	
5350	3	9	−20.76	0.78	167	0.82	17	0.51	0.19	
5905	3	12	−21.60	1.43	15	1.71	170	0.79	0.27	
5921	4	8	−20.67	1.19	180	1.26	350	0.50	0.29	
6907	4	12	−21.61	0.94	50	0.82	240	0.50	0.16	
7171	3	5	−20.03	0.39	50	0.61	200	0.38	0.11	
7412	3	9	−19.82	1.05	30	0.88	200	0.50	0.076	
7741	6	5	−18.76	1.04	235	1.08	50	0.48	0.26	
7755	5	4	−21.24	1.29	210	0.77	40	0.53	0.26	
IC 749.....	6	5	−18.39	0.56	187	0.75	7	0.52	0.11	

−0.045, in good agreement with the theoretical slope of −0.05. In Figure 4, the slope is −0.01. The correlation coefficients are low, 0.4 and 0.05, respectively.

In many galaxies, the inner two-arm spirals are particularly bright, narrow, and well defined (cf. Fig. 1). They appear to be intense ridges of star formation. Such spiral ridges were previously studied in more detail for NGC 4321 (EES) and NGC 1566 (Elmegreen & Elmegreen 1990). In both of these galaxies, the ends of the ridges are at corotation. Such ridges show up particularly well in the symmetric images of galaxies shown in EEM.

The statistical occurrence of ridges among galaxies of various types are as follows: for the 51 nonbarred grand-design (arm class 12) galaxies larger than 1′ radius and less inclined than 60° in the RC3, 27% have star formation ridges: 8 out of 22 (=36%) SA grand-design galaxies and 6 out of 29 (21%) SAB grand-design galaxies. For the 26 grand-design galaxies in the present sample, from Tables 1, 2, and 3 (which are larger

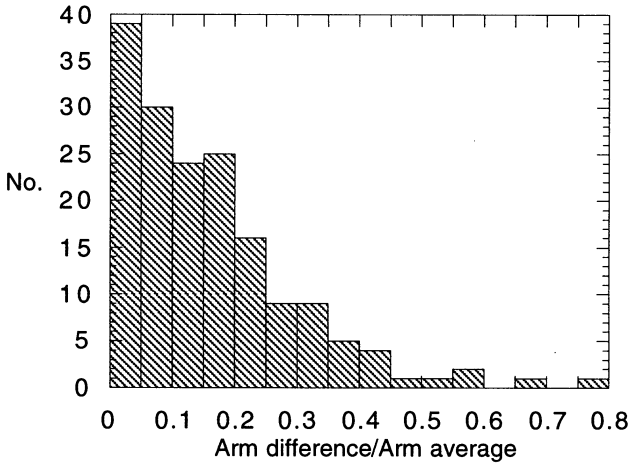

FIG. 2a

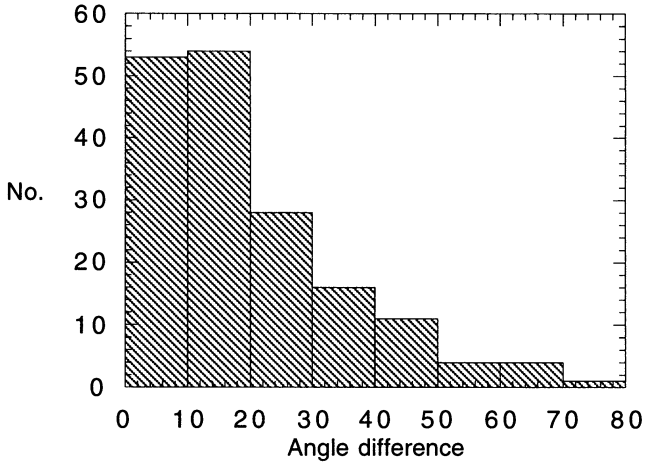

FIG. 2b

FIG. 2.—(*a*) Difference in corrected length between the two inner arms of a galaxy divided by the average length of the two arms is plotted in a histogram for all of the galaxies in this study. Most arms are the same length to within 20%. (*b*) Difference in the position angles of the endpoints of each arm with respect to the major axis (with 180° subtracted) is plotted in a histogram for all of the galaxies in this study. Most arms are symmetric to within 20°.

than 2.5 rather than 1'), 3/5 SAs, 7/10 SABs, and 3/11 SBs have ridges (all three SBs with ridges have large bars with flat light profiles), for a total of 13/26, or half. The occurrence of ridges is much less frequent in multiple-arm and flocculent galaxies, especially if they contain ovals or bars: for the 131 galaxies with multiple long-arm structure (arm classes 5–9) in Tables 1, 2, and 3, 9/37 SAs, 3/58 SABs, and 1/36 SBs have ridges for a total of 13/131, or 10%. For the flocculent galaxies in Tables 1, 2, and 3, 1/4 SAs, 1/8 SABs, and 0/7 SBs have ridges. Thus, ridges are very common (50%) in grand-design galaxies regardless of bar type, less common in nonbarred multiple-arm galaxies (24%), and uncommon in oval or barred multiple-arm galaxies and flocculent galaxies of any bar type.

The prominence of star formation ridges makes them useful as resonance indicators for grand-design galaxies; corotation lies close to the end of the ridge, about midway out to R_{25}. Figure 5 shows the relative radii of the endpoints of the spiral ridges for the nonbarred galaxies in our sample. The long-dashed line is for the inner 4:1 resonance, $R(\mathrm{I4{:}1})/R_{\mathrm{OLR}}$, and the solid line is for the corotation resonance, $R_{\mathrm{CR}}/R_{\mathrm{OLR}}$. The average ratio of the ridges' extent relative to R_{25} scatters around the ratio of $R_{\mathrm{CR}}/R_{\mathrm{OLR}}$. The slope of the data is -0.05, the same as the theoretical curve, with a correlation coefficient of 0.35.

Figures 6 and 7 show the relative lengths of the two symmetric arms for barred galaxies only (regardless of whether there are star formation ridges). Figure 6 has filled circles for R_{arm}/R_{25} in SB galaxies with small bars, $R_{\mathrm{bar}}/R_{25} < 0.3$, and Figure 7 has R_{arm}/R_{25} for SB galaxies with large bars, $R_{\mathrm{bar}}/R_{25} > 0.3$. Plus signs indicate the relative bar lengths, R_{bar}/R_{25}. The lines have the same convention as in Figures 3, 4, and 5. The galaxy types are divided into large and small bars because of an earlier suggestion (Elmegreen & Elmegreen 1985, 1989; Combes & Elmegreen 1993) that there are two types of bars, one type ending near corotation (i.e., the large bars, which have flat radial light distributions) and another type ending closer to the ILR (small bars, which have an exponential radial

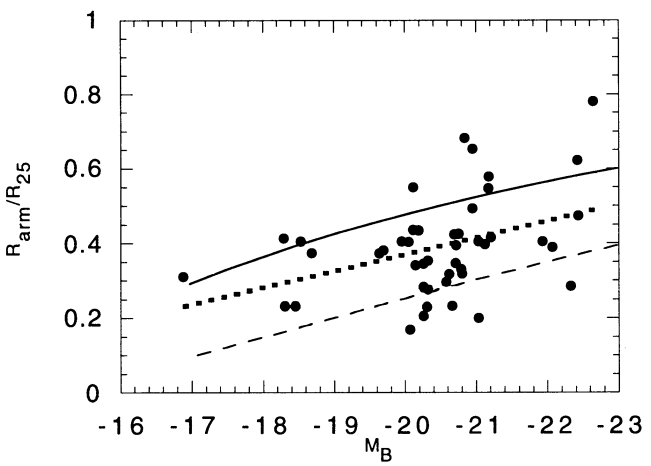

FIG. 3.—Average end of the two arms divided by R_{25} is plotted vs. absolute blue magnitude for SA galaxies, shown as circles in the figure. A least-squares fit is indicated by the short-dashed line. The solid line is the ratio of the corotation resonance to the OLR, and the long-dashed line is the ratio of the inner 4 : 1 resonance to the OLR.

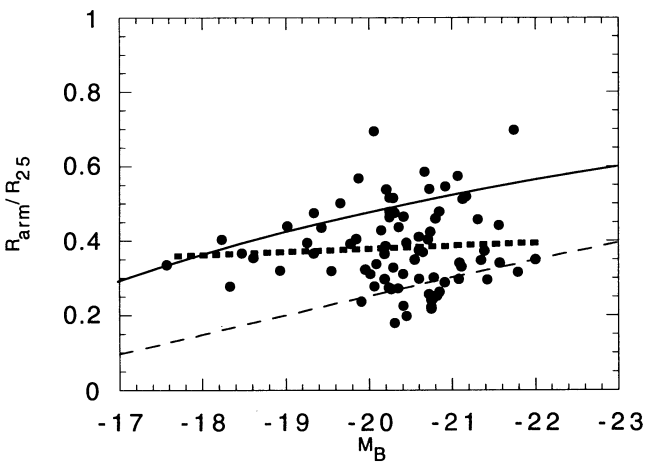

FIG. 4.—Average end of the two arms divided by R_{25} is plotted vs. absolute blue magnitude for SAB galaxies, shown as circles in the figure. The lines follow the same convention as in Fig. 3.

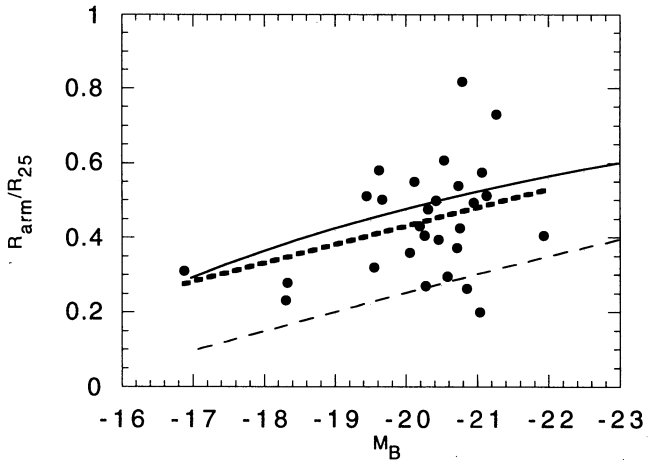

FIG. 5.—Average end of the two ridges divided by R_{25} is plotted vs. absolute blue magnitude for galaxies with star formation ridges. The lines follow the same convention as in Fig. 3.

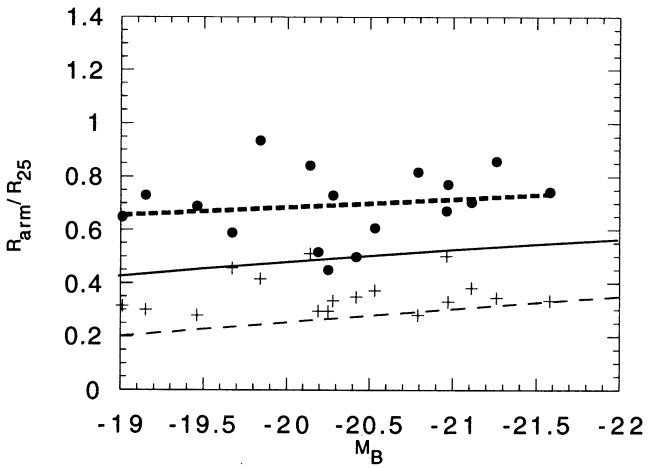

FIG. 7.—Average end of the two arms divided by R_{25} is plotted vs. absolute blue magnitude for large-bar SB galaxies, shown as circles in the figure. The bar radius divided by R_{25} is indicated by plus signs. The lines follow the same convention as in Fig. 3.

light distribution). Figures 6 and 7 indicate that both large and small bars occur over the whole magnitude range.

For small-bar SB galaxies (Fig. 6), the bars end at a radius less than or near the ultraharmonic (4:1) resonance, while the inner two-arm symmetric structure ends near corotation, just as in nonbarred galaxies; the two-arm slope is -0.05, the same as the theoretical curve, with a correlation coefficient of 0.38. For large-bar SB galaxies (Fig. 7), the bars end between the 4:1 radius and corotation, so the inner two arms end beyond this, at $\sim$80% of R_{25}; here the slope is 0.03, with a correlation coefficient of 0.1. In both cases, the overall spiral arm length is $\sim R_{25}$, which is probably near the OLR, as for the other galaxies studied in more detail elsewhere (EES; EEM).

In Figure 8, the average two-arm end, R_{arm}, divided by R_{25} is plotted versus the inclination-corrected bar radius, R_{bar}, divided by R_{25} for all barred galaxies. The dashed line shows the least-squares fit, which has a correlation coefficient of 0.7. The average end of the two arms scales with the bar radius; the two-arm structure always ends at about twice the bar radius. The correlation indicates that all barred galaxies are similar in their general bar-spiral morphology, despite the apparent differences in intrinsic bar properties.

The variation in relative spiral or bar radius with M_B was studied primarily because Persic & Salucci suggested that rotation curve slopes vary with M_B. When rotation curve slopes vary, ratios of resonance radii change too. In fact, the slight increase in R_{arm}/R_{25} or other quantities with galaxy luminosity could also result from a change with Hubble type, which is weakly correlated with M_B. Figure 9 shows this correlation for the galaxies in our sample. The sense of this correlation is such that early-type galaxies have larger R_{arm}/R_{25} than late-type galaxies. Instead of a resonance effect, this could result from other characteristics of a galaxy that are related to the mass distribution.

4. DISCUSSION

The identification with corotation of the bifurcation and broadening of the two inner symmetric arms of most spiral galaxies is a reasonable approximation that may be useful for dynamical studies of galaxies. For example, these features are not seen in most N-body simulations of spiral structure, which

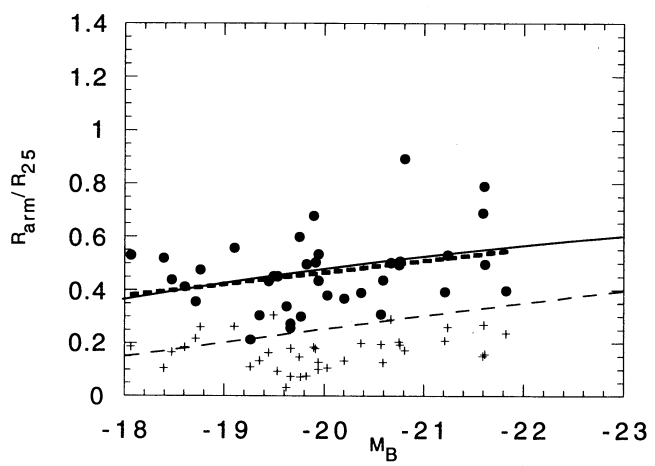

FIG. 6.—Average end of the two arms divided by R_{25} is plotted vs. absolute blue magnitude for small-bar SB galaxies, shown as circles in the figure. The bar radius divided by R_{25} is indicated by plus signs. The lines follow the same convention as in Fig. 3.

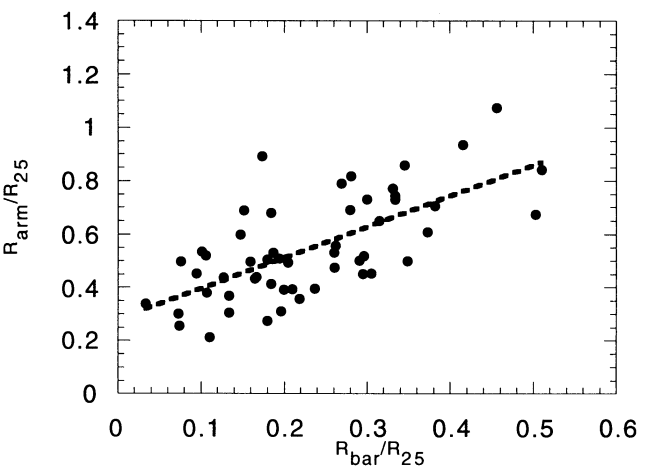

FIG. 8.—Average end of the two arms divided by R_{25} is plotted vs. the bar radius divided by R_{25} for all barred spirals.

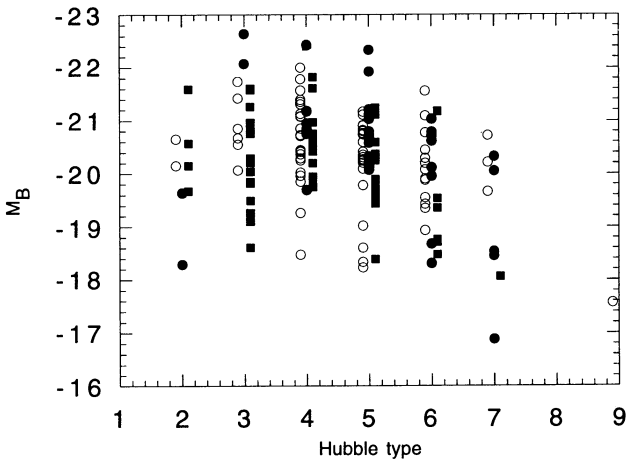

FIG. 9.—Absolute blue magnitudes for all of the galaxies in the sample are plotted vs. their Hubble types. Filled circles represent SA galaxies, open circles SAB galaxies, and filled squares SB galaxies.

suggests that the simulations are lacking some important physical processes in the inner regions, such as strong wave reflections or well-defined stellar orbits. The Patsis et al. (1994) simulations are an exception: they follow individual stellar orbits and find the observed break in spiral-arm continuity at corotation for strong spiral structure. They suggest that because of this, the spiral arms in real galaxies should end there (or at the inner 4:1 resonance for weaker arms), but we find here that only the strong symmetric parts of the arms end at corotation, with weaker or bifurcated arms extending beyond. Bifurcations and broadenings are also absent in *N*-body simulations of tidally generated spiral arms, possibly because these simulations do not follow individual stellar orbits, or because tidally generated spiral arms have corotation far out in their disks. For example, the interacting galaxies Arp 48 and 89 have two smooth arms that are continuous and nonbranching from the inner to the outer regions. However, some strongly interacting galaxies do show inner two-arm symmetry that leads to branching, as in Arp 65, 73, 74, 98, and 251 (Arp 1978); then corotation is presumably midway out in the disk.

The authors gratefully acknowledge support through NSF grant AST 92-01640.

REFERENCES

Arp, H. 1978, Atlas of Peculiar Galaxies (Pasadena: Caltech)
Buta, R. 1994, PASP, 105, 654
Buta, R., & Crocker, D. 1991, AJ, 102, 1715
Canzian, B. 1993, ApJ, 414, 487
Cepa, J., & Beckman, J. E. 1990a, ApJ, 349, 497
———. 1990b, A&A, 83, 211
Combes, F., & Elmegreen, B. G. 1993, A&A, 271, 391
de Vaucouleurs, G., de Vaucouleurs, A., Corwin, H. G., Jr., Buta, R., Paturel, G., & Fouqué, P. 1991, Third Reference Catalogue of Bright Galaxies (New York: Springer-Verlag) (RC3)
Elmegreen, B. G., & Elmegreen, D. M. 1985, ApJ, 288, 438
———. 1989, in Evolutionary Phenomena in Galaxies, ed. J. Beckman & B. Pagel (Cambridge: Cambridge Univ. Press), 83
———. 1990, ApJ, 355, 52
Elmegreen, B. G., Elmegreen, D. M., & Montenegro, L. 1992, ApJS, 79, 37 (EEM)
Elmegreen, B. G., Elmegreen, D. M., & Seiden, P. E. 1989, ApJ, 343, 602 (EES)
Elmegreen, D. M. & Elmegreen, B. G. 1982, MNRAS, 201, 1021
——. 1987, ApJ, 314, 3
Garcia-Burillo, S., Combes, F., & Gerin, M. 1993, A&A, 214, 148
Garcia-Burillo, S., Sempere, M. J., & Combes, F. 1994, A&A, 287, 419
Lin, C. C., & Shu, F. 1964, ApJ, 140, 656
Lowe, S. A., Roberts, W. W., Yang, J., Bertin, G., & Lin, C. C. 1994, ApJ, 247, 184
Patsis, P. A., Hiotelis, N., Contopoulos, G., & Grosbol, P. 1994, A&A, 286, 46
Persic, M., & Salucci, P. 1991, ApJ, 368, L60
Sandage, A. 1961, The Hubble Atlas of Galaxies (Washington, DC: Carnegie Inst. Washington)
Sandage, A., & Bedke, J. 1988, Atlas of Galaxies (Washington, DC: GPO)
Sandage, A., & Tammann, G. 1981, A Revised Shapley-Ames Catalog of Bright Galaxies (Washington, DC: Carnegie Inst. Washington) (RSA)
Saslaw, W. C. 1985, Gravitational Physics of Stellar and Galactic Systems (Cambridge: Cambridge Univ. Press)
Sempere, M. J., Garcia-Burillo, S., Combes, F., & Knapen, J. H. 1995, A&A, in press
Tully, R. B. 1988, Nearby Galaxies Catalog (Cambridge: Cambridge Univ. Press)
Westpfahl, D. 1995, ApJ, in press